npj | quantum materials

www.nature.com/npjquantmats

ARTICLE OPEN

Check for updates

Quantum phase transition in a clean superconductor with repulsive dynamical interaction

Dimitri Pimenov[1]✉ and Andrey V. Chubukov[1]

We consider a model of electrons at zero temperature, with a repulsive interaction which is a function of the energy transfer. Such an interaction can arise from the combination of electron–electron repulsion at high energies and the weaker electron–phonon attraction at low energies. As shown in previous works, superconductivity can develop despite the overall repulsion due to the energy dependence of the interaction, but the gap $\Delta(\omega)$ must change sign at some (imaginary) frequency ω_0 to counteract the repulsion. However, when the constant repulsive part of the interaction is increased, a quantum phase transition towards the normal state occurs. We show that, as the phase transition is approached, Δ and ω_0 must vanish in a correlated way such that $1/|\log[\Delta(0)]| \sim \omega_0^2$. We discuss the behavior of phase fluctuations near this transition and show that the correlation between $\Delta(0)$ and ω_0 locks the phase stiffness to a non-zero value.

npj Quantum Materials (2022)7:45 ; https://doi.org/10.1038/s41535-022-00457-3

INTRODUCTION

Understanding the nature of the "pairing glue", which enables Cooper pair formation of fermions, is one of the key steps toward a comprehensive scenario of superconductivity for a given material. In strongly correlated materials, like cuprates, iron-based, heavy-fermion, and organic materials, the attractive pairing interaction is likely of electronic origin. Near a quantum phase transition, such an attraction often takes a more concrete form of an effective four-fermion interaction, mediated by soft collective fluctuations of the corresponding order parameter. Most often, the attraction emerges in a channel different from an ordinary *s*-wave, in which case the superconductivity is labeled as an unconventional one.

For more conventional metals the symmetry of the pairing gap is *s*-wave, and the attraction is believed to come from electron–phonon interaction. This is the backbone of the "conventional" BCS theory of superconductivity. Still, to fully understand the phononic mechanism of *s*-wave superconductivity, one must explain why it is not overshadowed by the Coulomb repulsion, which is seemingly much larger. The frequently cited explanation[1–6] is that the repulsive Coulomb repulsion is logarithmically renormalized down between the Fermi energy E_F and the Debye energy Ω_D (the Tyablikov-McMillan logarithm), and at energies below Ω_D becomes smaller than the electron–phonon attraction, if the ratio E_F/Ω_D is large enough.

Upon closer examination, this explanation appears somewhat incomplete as Tyablikov-McMillan renormalization holds for the full interaction, i.e., for the sum of electron–electron and electron–phonon interactions, and under the renormalization this full interaction decreases, but does not change sign. It has been realized by several authors[4,7–12] that the underlying reason why electron–phonon superconductivity holds despite larger Coulomb interaction, is that the full interaction on the Matsubara axis (where it is real) is a dynamical one, $V(\Omega_m)$, and although a phonon-mediated attraction does not invert the sign of $V(\Omega_m)$, it nevertheless reduces it at frequencies below the Debye energy. It was argued that an "average" repulsive $V(\Omega_m)$ can be effectively eliminated from the equation for the pairing gap $\Delta(\omega_m)$, by choosing a solution which changes sign as a function of ω_m. This bears some similarity to how, for an electronic pairing, a static Coulomb repulsion is effectively eliminated by choosing a sign-changing, non-*s*-wave spatial structure of the gap function.

A convenient way to model the dynamical $V(\Omega_m)$, suggested in refs. [8–12], is to treat it as a sum of two parts: a constant repulsive part of strength f, representing the renormalized instantaneous Coulomb repulsion, and a frequency-dependent attractive part, due to electron–phonon interaction:

$$V(\Omega_m) \propto f - \frac{1}{1 + (\Omega_m/\Omega_1)^2}, \tag{1}$$

where Ω_1 is of order of the Debye energy. A similar reasoning has been applied[10] to dynamically screened electron–electron interaction, where Ω_1 is of the order of plasma frequency.

For $f > 1$, $V(\Omega_m) > 0$ for all frequencies, yet for $1 < f < f_c$, superconductivity emerges below a finite T_c, which contains f in the combination $f/[1 + \text{const.} \times f \log(E_F/\Omega_1)]$. For a given f and large enough $\log(E_F/\Omega_1)$, the Coulomb repulsion becomes logarithmically small, and one recovers the McMillan formula for T_c. One the other hand, at a given E_F/Ω_1, at large enough $f > f_c$, the repulsion becomes too strong and superconductivity vanishes. Obviously, T_c and the magnitude of the gap $\Delta(\omega_m)$ vanish at $f = f_c$.

It is the goal of the present work to understand the nature of the $T = 0$ quantum phase transition between a superconducting state at $f < f_c$ and a normal state at $f > f_c$. Specifically, we resolve the following puzzle: on the one hand, the gap $\Delta(\omega_m)$ must change sign at some finite $\omega_m = \omega_0$, otherwise there would be no solution of the gap equation for $f > 1$. On the other hand, for any finite ω_0, $\Delta(0)$ is non-zero, in which case the linearized gap equation does not have a solution as the pairing kernel contains an infrared-divergent Cooper logarithm, which is not regularized at $T = 0$ and therefore does not admit a solution. We argue analytically and check numerically that as f approaches f_c from below, $\omega_0 \to 0$ and $\Delta \to 0$ in tune with each other, such that $1/|\log \Delta| \sim \omega_0^2$.

We also analyze the spectrum of gapless phase fluctuations near $f = f_c$. We show that because of the relation between Δ and

[1]William I. Fine Theoretical Physics Institute, University of Minnesota, Minneapolis, MN 55455, USA. ✉email: dpimenov@umn.edu

ω_0, the superfluid stiffness remains finite as f approaches f_c from below. This is in marked contrast with the behavior of the stiffness near the end point of superconductivity at $T=0$ in a system with magnetic impurities (Abrikosov-Gorkov theory, refs. [13–16]). In this situation, the destruction of superconductivity occurs via pair-breaking due to the impurity-induced self-energy, and the superfluid stiffness gradually vanishes as the system approaches the $T=0$ phase transition.

That superconductivity vanishes when $\omega_0=0$ can also be interpreted from a topological viewpoint, because $\omega_m=\omega_0$ is a center of a dynamical vortex: the anti-clockwise circulation of the phase of $\Delta(z)$, $z=\omega'+i\omega''$, around this point is 2π, refs. [17–19]. There is no way to eliminate this dynamical vortex as there are no anti-vortices in the upper half-plane of frequency (their presence would be incompatible with the analyticity of $\Delta(z)$). Hence, as long as superconducting order is present, ω_0 must remain finite. The only possibility for a vortex to disappear without destroying superconductivity is when it moves to an infinite frequency. For the model of Eq. (1) this holds at $f=0$, and for $f<0$ the gap function $\Delta(\omega_m)$ on the Matsubara axis is nodeless.

We note in passing that a vortex on the Matsubara axis gives rise to 2π winding of the phase of $\Delta(\omega)$ on the real frequency axis, between $\omega=-\infty$ and $\omega=\infty$. Such phase winding necessary leads to nodes in the real and imaginary parts of $\Delta(\omega)$, which can be detected by spectroscopic experiments, e.g., ARPES[20].

RESULTS

Model

We consider a spatially isotropic model of interacting spin-1/2 fermions at zero temperature in d dimensions, described by the effective low-energy action

$$\begin{aligned}\mathcal{S}=&\sum_\sigma\int_k\bar\psi_\sigma(k)(i\omega-\xi_{\mathbf{k}})\psi_\sigma(k)\\&+\int_{k,k',q}V(\omega-\omega')\times\bar\psi_\uparrow(k'+q/2)\bar\psi_\downarrow(-k'+q/2)\\&\psi_\downarrow(-k+q/2)\psi_\uparrow(k+q/2)\,,\int_k=\int_{-\Lambda}^{\Lambda}\frac{d\omega}{2\pi}\int\frac{d\mathbf{k}}{(2\pi)^d}\,,\end{aligned}\tag{2}$$

where Λ is a UV cutoff of order E_F and ω are Matsubara frequencies (here and below we label Matsubara frequency as ω without subscript m). The interaction $V(\Omega)$ is taken to be a function of the energy transfer, but independent of momenta. We follow earlier works[9–12,21] and set $V(\Omega)$ to

$$V(\Omega)=\frac{2}{\rho}\times\tilde V(\Omega),\quad \tilde V(\Omega)=\lambda\left(f-\frac{1}{1+(\Omega/\Omega_1)^2}\right),\tag{3}$$

where ρ is the single-spin density of states at the Fermi surface, and Ω_1 is of the order of Debye energy for the electron–phonon case (the factor of 2 is introduced for notational convenience).

In the following, we measure all energies in units of Ω_1, and hence set $\Omega_1=1$ in Eq. (3). Then, $\Lambda\gg1$. A discussion of the opposite low-density limit where E_F, $\Lambda\ll1$ can be found in ref. [22]. For the known physical realizations of Eq. (3), $f>1$, hence $V(\Omega)$ remains positive (repulsive) at all frequencies. For completeness, here we consider arbitrary f, but our key focus will still be on $f>1$. For a generic f, $V(\Omega)$ is purely attractive for $f\le0$, is attractive at small frequencies and repulsive at large frequencies for $0<f<1$, and is purely repulsive for $f\ge1$, see Fig. 1a. The dimensionless λ parametrizes the overall strength of the interaction. We assume $\lambda\le1$, this will allow us to neglect, at least qualitatively, the normal fermionic self-energy: One can show that the leading self-energy effect is a mere renormalization of the coupling constant $\lambda\to\lambda/(1+2\lambda)$.

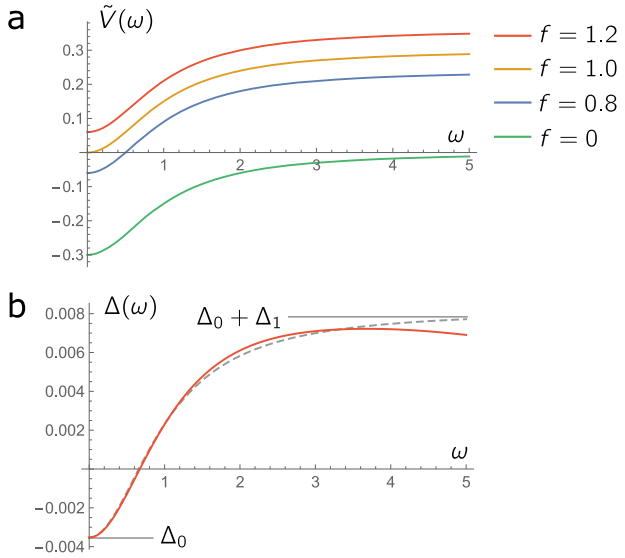

Fig. 1 Dynamical interaction and typical gap function. a $\tilde V(\omega)$ for $\Lambda=5$, $\lambda=0.3$ and four different values of f. **b** Numerical solution of the gap equation for $f=1.2$. Gray dashed line corresponds to a fit to $\Delta(\omega)$ using the ansatz (11).

Gap equation

To describe superconductivity, we perform a Hubbard-Stratonovich transformation in the spin-singlet, s-wave pairing channel and use a saddle point approximation. This procedure leads to the conventional Eliashberg equation for the gap function[23], though without the additional contribution from the self-energy. On the Matsubara axis, we have

$$\Delta(\omega)=-\int_{-\Lambda}^{\Lambda}d\omega'\frac{\Delta(\omega')\tilde V(\omega-\omega')}{\sqrt{(\omega')^2+|\Delta(\omega')|^2}}\,.\tag{4}$$

The interaction $\tilde V(\omega-\omega')$ is real on the Matsubara axis, which allows us to set $\Delta(\omega)$ to be real by properly choosing its phase. At the same time, because the interaction is a function of the frequency transfer, one can search for even-frequency and odd-frequency $\Delta(\omega)$. In this communication, we focus on the even-frequency solutions. For even-frequency $\Delta(\omega)=\Delta(-\omega)$, the gap equation can be rewritten as

$$\Delta(\omega)=-\int_0^{\Lambda}d\omega'\frac{\Delta(\omega')\left[\tilde V(\omega-\omega')+\tilde V(\omega+\omega')\right]}{\sqrt{(\omega')^2+\Delta(\omega')^2}}\,.\tag{5}$$

It is obvious that for $f>1$, when $\tilde V>0$, $\Delta(\omega)$ must change sign at some frequency ω_0 as otherwise the left-hand side and the right-hand side of Eq. (5) would have opposite signs. The value of ω_0 is chosen to minimize the effect of a repulsive f in Eq. (3). This has been discussed before[2–6,8,11,12] and we just state the results. First, ω_0 is finite for all $f>0$ if $\Lambda<\infty$. If Λ is finite, $\Delta(\omega)$ has a node as long as $\omega_0<\Lambda$. Second, optimizing ω_0 in the limit $\log(\Lambda)\gg1$, one obtains that a repulsive f effectively gets reduced to $f/[1+\lambda f\log(\Lambda)]\to1/\lambda\log(\Lambda)$. This gives rise to the McMillan formula for $T_c\propto e^{-1/(\lambda-\mu^*)}$, in which $\mu^*\approx1/\log\Lambda$ is the contribution from the repulsion. Third, for any finite Λ, the repusive part of the interaction gets reduced, but cannot be completely eliminated. As a result, superconductivity exists at f smaller than some critical $f_c>1$.

In Fig. 1b we present the numerical solution of the non-linear gap equation (5) for some representative Λ and $1<f<f_c$. We clearly see that $\Delta(\omega)$ changes sign at some finite ω_0. It reaches a finite value at $\omega=0$ and then saturates at some other finite value, of opposite sign at $\omega_0\ll\omega<\Lambda$. The numerical solution has been

obtained by a "damped iteration" method, in which only a certain portion of $\Delta(\omega)$ is updated at each step of iterations. This method improves the convergence of the iteration procedure[12].

Quantum phase transition towards a superconductor with nodeless $\Delta(\omega)$

Before we proceed to the case $f \approx f_c$, we briefly discuss the transition towards the state with a nodeless $\Delta(\omega)$. As stated above, this transition occurs at $f = 0$ when $\Lambda = \infty$, i.e., Eq. (5) holds at all frequencies. This transition can be classified as topological because it separates two states with and without a dynamical vortex. As f is reduced towards $f = 0$, ω_0 increases, i.e., the core of the dynamical vortex successively moves to larger ω. At $f = 0$ it reaches $\omega = \infty$ and disappears.

We now argue that the dependence of ω_0 of f has a simple form

$$\omega_0 = f^{-1/2} \quad \text{as} \quad f \to 0\,. \tag{6}$$

This can be obtained as follows: Let $\Delta_a(\omega)$ be the solution of the gap equation at $f = 0$:

$$\Delta_a(\omega) = \lambda \int_0^\Lambda d\omega' \left(\frac{1}{1+(\omega-\omega')^2} + \frac{1}{1+(\omega+\omega')^2}\right) \times \frac{\Delta_a(\omega')}{\sqrt{(\omega')^2+\Delta_a(\omega')^2}}\,. \tag{7}$$

Since $\tilde{V}(\omega)$ is purely attractive for $f = 0$, Δ_a has a fixed sign. At large ω, $\Delta_a(\omega) = A/\omega^2$, where

$$A = 2\lambda \int_0^\Lambda d\omega' \frac{\Delta_a(\omega')}{\sqrt{(\omega')^2 + \Delta_a(\omega')^2}}\,. \tag{8}$$

Now let $\Delta_b(\omega)$ be the solution of the gap equation at small but finite f. To the leading order in f, we obtain, for large ω,

$$\Delta_b(\omega) \simeq \Delta_a(\omega) - Af = A\left(\frac{1}{\omega^2} - f\right). \tag{9}$$

At the node, $\Delta_b(\omega_0) = 0$, hence $\omega_0 = f^{-1/2}$. For large but finite Λ, the phase transition occurs when $\omega_0 = \Lambda$. The corresponding critical f for a topological transition is then

$$f_{c,\text{top}} = \Lambda^{-2}\,. \tag{10}$$

In Fig. 2 we checked these results by solving the gap equation numerically. The agreement between the numerical and analytical results is perfect.

Quantum phase transition towards normal state

We now consider the system behavior near the $T = 0$ transition towards the normal state at $f = f_c > 1$, when the pairing interaction $V(\omega - \omega')$ is positive (repulsive) at all frequencies. We assume and then verify that the transition is continuous, i.e., at $f = f_c - 0^+$, $\Delta(\omega)$ is infinitesimally small. Like we said in the Introduction, to understand this transition one has to resolve the following puzzle: if infinitesimally small $\Delta(\omega)$ tends to a finite value at $\omega = 0$, like, e.g., in Fig. 1b, the right-hand side of the linearized gap equation gives rise to a divergent Cooper logarithm. Because $T = 0$, the logarithmical divergence is not cut. The only way to avoid this divergence is to place the node (i.e., the vortex core) right at $\omega = 0$. But then the gap becomes sign-preserving at all finite ω, and for such $\Delta(\omega)$ there is no solution of the gap equation for a purely repulsive interaction.

As we now show, the resolution of this problem is to let both Δ and ω_0 vanish in a correlated way as $f \to f_c$ from below. To simplify the analysis, we first note that for all $f < f_c$, the gap function $\Delta(\omega)$ is well approximated by a simple form

$$\Delta(\omega) = \Delta_0 + \Delta_1 \frac{\omega^2}{1+\omega^2}\,. \tag{11}$$

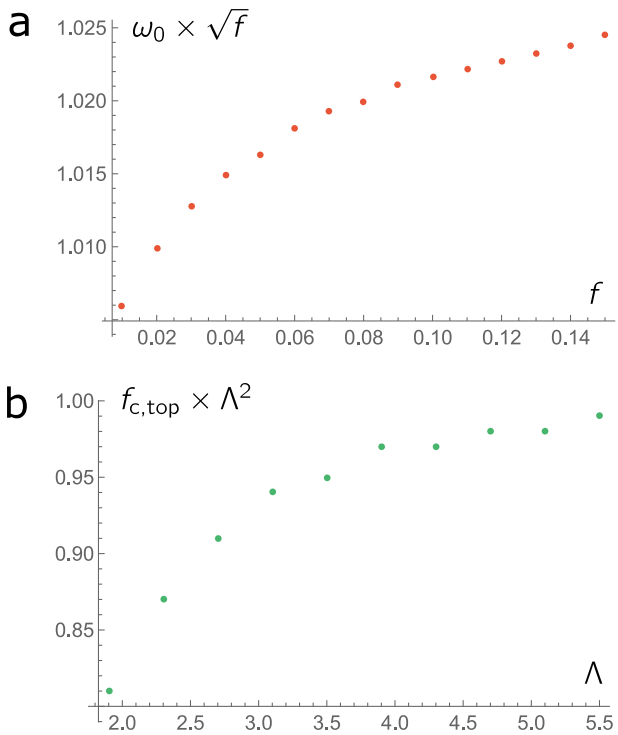

Fig. 2 Scaling behavior at the transition towards the nodeless superconductor. a Numerical check of Eq. (6) for small f. **b** Numerical check of Eq. (10) for moderate Λ. The apparent oscillations are due to discretization of f in the numerics. Used parameter: $\lambda = 0.1$.

A comparison with the numerical solution of the gap equation shows that this form is near-perfect for $\omega < 1$ and matches the numerical results reasonably well for $\omega > 1$, see Fig. 1b. Such agreement is sufficient to extract the leading behavior near the phase transition (see below). The coefficients Δ_0, Δ_1 can be determined by inserting the ansatz (11) into (5) and expanding up to second order in ω. After a straightforward algebra we obtain

$$\Delta_0 = -2\lambda \int_0^\Lambda d\omega' \left(f - \frac{1}{1+(\omega')^2}\right) \times K(\omega') \tag{12}$$

$$\Delta_1 = 2\lambda \int_0^\Lambda d\omega' \frac{\left(3(\omega')^2 - 1\right)}{\left(1+(\omega')^2\right)^3} \times K(\omega') \tag{13}$$

$$K(\omega') = \frac{\Delta_0 + \Delta_1 \frac{(\omega')^2}{1+(\omega')^2}}{\sqrt{(\omega')^2 + \left(\Delta_0 + \Delta_1 \frac{(\omega')^2}{1+(\omega')^2}\right)^2}}\,. \tag{14}$$

In the limit $\Delta_0, \Delta_1 \to 0$, the equations simplify to

$$\begin{aligned} \Delta_1 &= \tfrac{\Delta_1 \lambda}{6} - 2\lambda\ell\Delta_0 \\ \Delta_0 &= \Delta_0[-2\lambda f L - 2\lambda\ell(f-1)] + \Delta_1(-2\lambda f L + \lambda) \end{aligned}\,, \tag{15}$$

where

$$L = \log(\Lambda),\ \ \ell = \log(1/\Delta_0) \gg L \tag{16}$$

The value of the critical f_c can be determined by evaluating the determinant of the set (15) in the limit $\ell \to \infty$. We obtain

$$f_c = \frac{1 - 7/6 \times \lambda}{1 - \lambda/6 - 2L\lambda}\,. \tag{17}$$

The divergence of f_c at a critical value of λL, which is evident from Eq. (17) is not an artifact of the approximation to $\Delta(\omega)$, as we have checked numerically. Rather, it implies that by properly

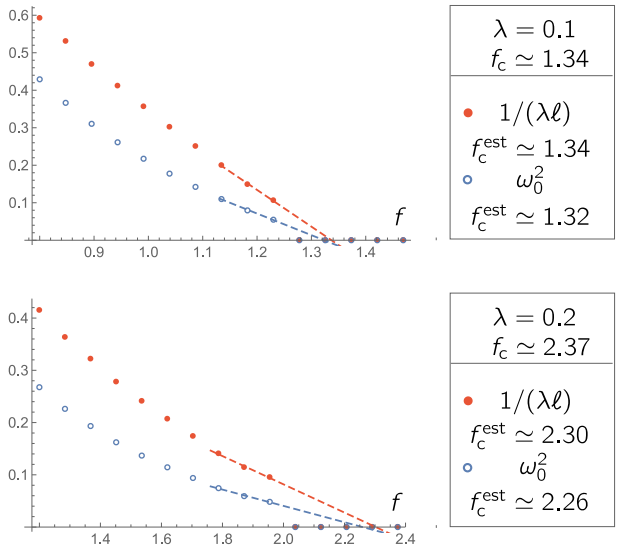

Fig. 3 Scaling behavior at the transition towards the normal state. Evolution of $1/(\lambda\ell)$ (filled circles) and ω_0^2 (empty circles) close to the phase transition; both quantities vanish with approximately constant slope (i.e., are $\propto f_c - f$), as expected from Eqs. (19) and (21). Values f_c^{est} shown in the plot legend are derived from linear extrapolation of the last three data points (dashed lines), showing semi-quantitative agreement with f_c from Eq. (17).

placing ω_0, one can completely eliminate a constant repulsion f even when f is large. A detailed analysis of this effect will be presented elsewhere (in preparation).

The general trend that f_c increases with increasing Λ is also in agreement with McMillan reasoning that the Coulomb repulsion is suppressed at large Λ. In the following, we focus on $\lambda L \ll 1$, in which case

$$f_c = 1 + \lambda(2L-1) + \mathcal{O}((\lambda L)^2) \tag{18}$$

Evaluating the determinant again, but this time for a finite ℓ, we obtain to leading order in λL and $f_c - f$:

$$\ell \simeq \frac{1}{2\lambda(f_c - f)} \times \left(\frac{1}{1-2\lambda L}\right)^2 \tag{19}$$

Using (16) we find that $\Delta_0 = \exp(-\ell)$ vanishes exponentially fast as $f \nearrow f_c$.

From the first equation in (15) we obtain

$$\frac{\Delta_0}{\Delta_1} \simeq -\frac{1}{2\lambda\ell} \simeq -(f_c - f)(1-2\lambda L)^2 . \tag{20}$$

The ratio is negative (hence ω_0 is finite) and progressively decreases when f approaches f_c. Substituting Δ_0/Δ_1 into (11), we obtain

$$\omega_0 \simeq \sqrt{f_c - f} \times (1 - 2\lambda L). \tag{21}$$

We see that ω_0 vanishes as $\sqrt{f_c - f}$, i.e., much more gradually than Δ_0.

In Fig. 3, we verify the scaling forms of Δ_0 and ω_0 by extracting these two quantities from the numerical solution of the gap equation. The agreement between analytical and numerical results is quite good.

Phase fluctuations near critical f_c

For a more detailed characterization of the phase transition at $f = f_c$, we now look at soft collective excitations in the system. These are phase fluctuations, which in the absence of long-range Coulomb interaction are Goldstone modes of the superconducting state. Our goal is to derive the superfluid density and the

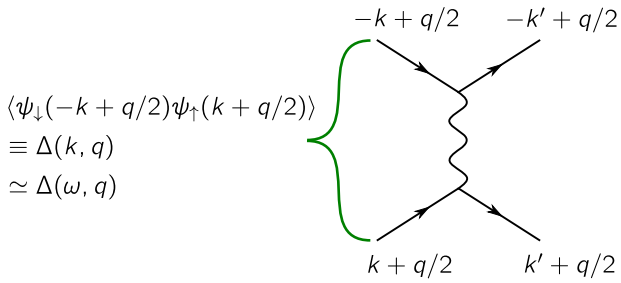

Fig. 4 Energy-momentum dependence of the pairing field Δ. The brace represents the Hubbard-Stratonovich decoupling. Four-momenta $k = (\omega, \mathbf{k})$, $q = (\Omega, \mathbf{q})$ are used. We always neglect the dependence of Δ on the relative momentum of a Cooper pair, $\mathbf{k}$.

dynamical compressibility, which enter the propagator of phase fluctuations, as functions of $q = (\Omega, \mathbf{q})$, where $\mathbf{q}$ the total momentum of a Cooper pair and Ω is the total frequency. There are two ways to do this: either expand the action to second order in θ or analyze the pole structure of the full particle–particle susceptibility at small q. These two methods yield consistent results; we will focus on the first one in the remainder of this section as we discuss the other one in the "Methods" section.

To obtain the propagator of low-energy phase fluctuations, we introduce the total momentum $\mathbf{q}$ and the total frequency Ω of a Cooper pair. For convenience, we combine $\mathbf{q}$ and Ω into a $(d+1)$-dimensional variable $q = (\Omega, \mathbf{q})$. In our mean-field solution the pairing involves fermions with frequencies ω and $-\omega$ and momenta $\mathbf{k}$ and $-\mathbf{k}$, i.e., q is set to zero. In other words, the mean-field gap is a function of ω but not of q. This mean-field solution corresponds to a minimum of the Luttinger-Ward functional. States away from the minimum are described by a fluctuating pairing field (order parameter) that depends on both Ω and q. We illustrate this in Fig. 4.

Low-energy fluctuations around the mean-field solution correspond to slow variations of the phase of the order parameter $\theta(q)$:

$$\begin{aligned}\Delta(\omega,q) &\simeq \Delta(\omega) \times \left[\delta^{(d+1)}(q) + i\theta(q)\right] \\ \bar{\Delta}(\omega,q) &\simeq \Delta(\omega) \times \left[\delta^{(d+1)}(q) - i\theta(-q)\right].\end{aligned} \tag{22}$$

The expressions in the square brackets arise from small-θ expansion and Fourier transformation of the real-space phase factor

$$\begin{aligned}&\int \frac{d^{d+1}q}{(2\pi)^{d+1}} \exp[i\theta(x)] \exp[i(x\cdot q)] \simeq \\ &\int \frac{d^{d+1}q}{(2\pi)^{d+1}} (1 + i\theta(x)) \exp[i(x\cdot q)] = \delta^{(d+1)}(q) + i\theta(q)\end{aligned} \tag{23}$$

where x is the center-of-mass coordinate.

Inserting the expansion (22) into the Δ-dependent action, where the fermions have been integrated out, and expanding to the second order in θ, we obtain the following action for the θ field (see "Methods" for details):

$$\begin{aligned}\mathcal{S}_\theta = &\int \frac{d\Omega}{2\pi} \frac{d\mathbf{q}}{(2\pi)^d} \theta(q)\theta(-q) \\ &\left[\int \frac{d\omega d\omega'}{(2\pi)^2} \Delta(\omega)(-V^{-1})(\omega-\omega')\Delta(\omega') - \Pi_\Delta(q)\right].\end{aligned} \tag{24}$$

$$\Pi_\Delta(q) = \int \frac{d\omega}{2\pi} \frac{d\mathbf{k}}{(2\pi)^d} \frac{\Delta^2(\omega)}{\omega_+^2 + E_+^2} \frac{1}{\omega_-^2 + E_-^2} \times [\Delta_+\Delta_- + (i\omega_+ + \xi_+)(i\omega_- + \xi_-)],$$
$$\xi_\pm = \xi_{\mathbf{q}/2\pm\mathbf{k}}, \omega_\pm = \Omega/2 \pm \omega, \Delta_\pm = \Delta(\omega_\pm), E_\pm = \sqrt{(\Delta_\pm)^2 + (\xi_\pm)^2}. \tag{25}$$

Here, $V^{-1}(\omega-\omega')$ is the inverse of $V(\omega-\omega')$ defined by

$$\int \frac{d\omega_1}{2\pi} V(\omega-\omega_1)V^{-1}(\omega_1-\omega') = 2\pi\delta(\omega-\omega'). \tag{26}$$

The expression for $\Pi_\Delta(q)$ in Eq. (24) can directly be obtained from the expansion in θ. Alternatively, it can be obtained diagrammatically as a particle–particle bubble with form-factors $\Delta^2(\omega)$ (see "Methods").

Multiplying both sides of Eq. (4) by $V^{-1}(\omega-\tilde{\omega})\Delta(\tilde{\omega})$ and integrating over $\omega,\tilde{\omega}$ we find that

$$\int \frac{d\omega d\omega'}{(2\pi)^2}\Delta(\omega)(-V^{-1})(\omega-\omega')\Delta(\omega') = \frac{\rho}{2}\int d\omega \frac{\Delta(\omega)}{\sqrt{\Delta(\omega)^2+\omega^2}} \tag{27}$$

This expression coincides with the particle–particle bubble in the limit of vanishing q:

$$\begin{aligned}\Pi_\Delta(0) &= \rho\int\frac{d\omega}{2\pi}d\xi\frac{\Delta(\omega)^2}{\Delta(\omega)^2+\xi^2+\omega^2}\\ &= \frac{\rho}{2}\int d\omega\frac{\Delta(\omega)}{\sqrt{\Delta(\omega)^2+\omega^2}}.\end{aligned} \tag{28}$$

As a result, the propagator of the field $\theta(q)$ is determined by $\Pi_\Delta(q) - \Pi_\Delta(0)$. Expanding $\Pi_\Delta(q)$ to second order in Ω, $\mathbf{q}$, we obtain

$$S_\theta \simeq \frac{\rho}{4}\int\frac{d\Omega}{2\pi}\frac{d\mathbf{q}}{(2\pi)^2}\theta(q)\theta(-q)\left[\frac{1}{d}n_s|v_F\mathbf{q}|^2+\kappa\Omega^2\right]. \tag{29}$$

The coefficient n_s in the second line of (29) is the superfluid density, normalized by the density of electrons in the normal state.

It parametrizes the energy cost of spatial phase fluctuations of the order parameter and controls the supercurrent and magnetic response in the superconducting state (The prefactor $1/d$ comes from averaging over $\cos[(\mathbf{k},\mathbf{q})]^2$ in d dimensions). The factor κ is a dynamical compressibility which parametrizes the energy cost of temporal phase fluctuations. We find

$$n_s = \frac{1}{2}\int_{-\Lambda}^{\Lambda}d\omega\frac{\Delta(\omega)^2}{(\Delta(\omega)^2+\omega^2)^{3/2}} \tag{30}$$

$$\begin{aligned}\kappa = &\tfrac{1}{4}\textstyle\int_{-\Lambda}^{\Lambda}d\omega\frac{\Delta(\omega)^2}{(\Delta(\omega)^2+\omega^2)^{5/2}}\\ &\times\left[\Delta(\omega)^2(3-\Delta(\omega)\Delta(\omega)'')+\omega^2(-\Delta(\omega)\Delta''(\omega)+3\Delta'(\omega)^2)\right].\end{aligned} \tag{31}$$

where the derivatives are with respect to ω. A similar expression for n_s was also obtained in ref. [24].

For a weakly frequency-dependent $\Delta(\omega)$, the expressions for n_s and κ are the same as in BCS theory, $n_s=\kappa=1$. For a generic $\Delta(\omega)$, the BCS results are correct by order of magnitude, but the actual values of n_s and κ differ by BCS expressions by $O(1)$, see Fig. 5.

At $f\le f_c$, $\Delta(\omega)$ is exponentially small, and the integrals are dominated by $\omega\lesssim\Delta(0)$. Because frequency variation of $\Delta(\omega)$ occurs at a much larger scale $\omega_0\gg\Delta(0)$, the gap in (30) and (31) can be approximated by a constant $\Delta(0)$. As a result, both n_s and κ tend to BCS values $n_s=\kappa=1$. We verified this result in numerical calculations, see Fig. 5. The velocity of phase fluctuations also approaches the BCS value

$$v_s \to \frac{1}{\sqrt{d}}v_F \quad \text{for} \quad f\nearrow f_c. \tag{32}$$

At $f=f_c+0^+$, n_s and κ jump to zero.

We emphasize that the behavior of n_s near the $T=0$ superconductor-normal state phase transition in a clean system at $f=f_c$ is different from the one at the $T=0$ superconductor-normal state phase transition due to magnetic impurities. There, n_s gradually vanishes at a critical impurity concentration due to pair-breaking coming from the impurity-induced self-energy. As a result, the penetration depth $\sim 1/\sqrt{n_s}$ diverges (refs. [13,14,16]). At a technical level, this is because in the case of magnetic impurities the denominator of Eq. (30) contains an additional term proportional to the fermionic damping rate due to impurity scattering. In our case, such a constant term is absent. We expect, however, that it will appear if we extend the analysis of the superconductor-normal state phase transition to a finite magnetic field H. We therefore expect that at a finite field, n_s will vanish at critical $f_c(H)$.

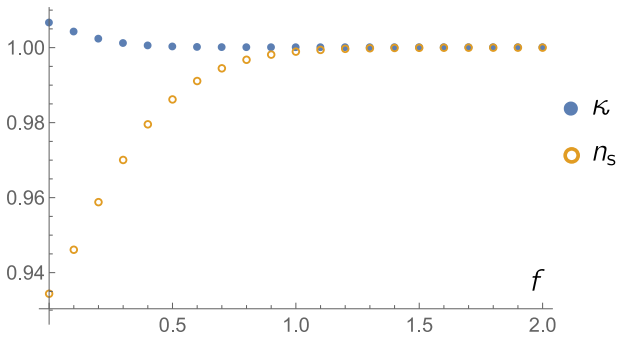

Fig. 5 Normalized compressibility and superfluid density. κ and n_s are shown as function of f. Used parameters: $\lambda=0.3$, $\Lambda=5$.

Still, the discontinuity of n_s at $f=f_c$ in our case holds only for superfluid density evaluated at zero momentum $\mathbf{q}$, or, more accurately, at $|v_F\mathbf{q}|\ll\Delta_0$. To analyze the behavior at larger $|\mathbf{q}|$, we define a generalized momentum-dependent superfluid density as

$$n_s(\mathbf{q}) \equiv \frac{(\Pi_\Delta(0)-\Pi_\Delta(\mathbf{q},0))}{\frac{\rho}{4d}|v_F\mathbf{q}|^2}. \tag{33}$$

This $n_s(\mathbf{q})$ is a scaling function of $\tilde{q}=v_F|\mathbf{q}|/\Delta(0)$. The form of the scaling function depends on the dimensionality. In 2D we have

$$n_s^{2D}(\mathbf{q}) \simeq \int_{-\infty}^{\infty}dx\frac{1}{\frac{1}{4}\tilde{q}^2}\times\left[\frac{1}{\sqrt{1+x^2}}-\frac{1}{\sqrt{1+x^2+\frac{1}{4}\tilde{q}^2}}\right], \tag{34}$$

where we have approximated $\Delta(\omega)\simeq\Delta(0)$ and $\Lambda/\Delta(0)=\infty$, which holds to a good numerical accuracy. Evaluating the frequency integral we find:

$$n_s^{2D}(\tilde{q}) = \frac{1}{\frac{1}{4}\tilde{q}^2}\log\left(1+\frac{1}{4}\tilde{q}^2\right). \tag{35}$$

In 3D we have

$$\begin{aligned}n_s^{3D}(\tilde{q}) &= \tfrac{12}{\tilde{q}^3}\textstyle\int dx\left[\frac{\tilde{q}/2}{\sqrt{x^2+1}}-\arctan\left(\frac{\tilde{q}/2}{\sqrt{x^2+1}}\right)\right]\\ &= \tfrac{12}{\tilde{q}^3}\left[\sqrt{4+\tilde{q}^2}\times\operatorname{arctanh}\left(\frac{\tilde{q}}{\sqrt{4+\tilde{q}^2}}\right)-\tilde{q}\right].\end{aligned} \tag{36}$$

We plot $n_s^{2D}(\tilde{q})$ and $n_s^{3D}(\tilde{q})$ in Fig. 6a. We see that both functions decrease with increasing $\tilde{q}$, i.e., with decreasing Δ_0 for a given $\mathbf{q}$. At $f=f_c-0^+$, $n_s^{2D,3D}(\tilde{q})$ vanishes for any finite $\mathbf{q}$. A suitably defined momentum-dependent compressibility $\kappa(\mathbf{q})\sim\partial^2\Pi_\Delta(\Omega,\mathbf{q})/\partial\Omega^2|_{\Omega=0}$ follows the same trend (Fig. 6b). This behavior is indeed fully expected as for $|v_F\mathbf{q}|\gg\Delta(0)$, the system is effectively in the normal state, where the $U(1)$ symmetry is preserved and gauge (phase) fluctuations do not cost any energy.

DISCUSSION

In this communication, we analyzed a $T=0$ superconductor-normal state transition for a model of fermions coupled by a frequency-dependent interaction $V(\Omega)$, which has a repulsive constant part f and an Ω-dependent attractive part. For $f<0$, $V(\Omega)$ is fully attractive, and the system displays a conventional s-wave

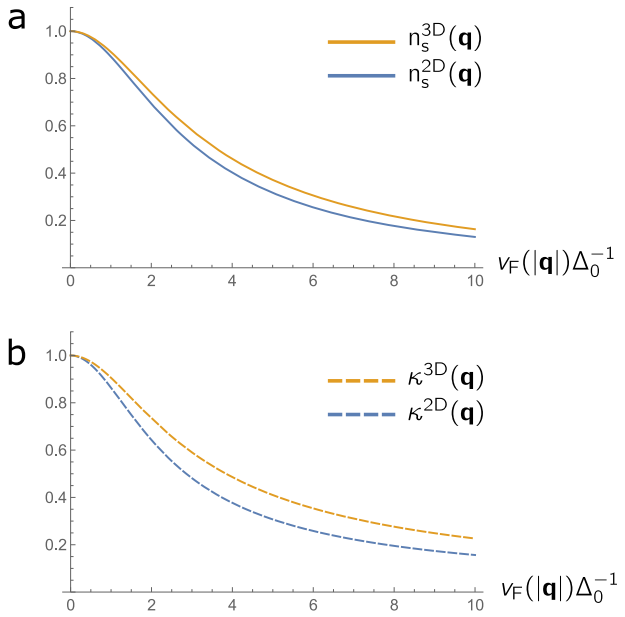

Fig. 6 Generalized superfluid density. a $n_s(\mathbf{q})$ determined from Eqs. (35) and (36), **b** $\kappa(\mathbf{q})$, obtained in the same way as $n_s(\mathbf{q})$.

superconductivity with a sign-preserving $\Delta(\omega)$ along the Matsubara axis. At $0 < f < 1$, the interaction $V(\Omega)$ is attractive at small frequencies, but repulsive at large Ω. In this case, superconductivity is still present at $T = 0$, but the gap function has a node along the Matsubara axis, at some finite $\omega = \omega_0$. Because a nodal point of $\Delta(\omega)$ is a center of a dynamical vortex, the superconducting states at $f < 0$ and at $f > 0$ are topologically different. We analyzed the topological transition at $f = 0$ and argued that the vortex emerges at an infinite frequency at $f = 0$ and moves to a finite ω_0 at a finite f. This is an expected behavior, consistent with earlier analysis of a similar model[17]. We also analyzed how the critical f for such topological transition changes if we set a finite UV cutoff for the interaction.

The superconducting state with a sign-changing $\Delta(\omega)$ persists also for $f > 1$, when $V(\Omega)$ becomes positive at all frequencies, and vanishes at a finite f_c. The key part of our work is the analysis how the gap function Δ and the frequency ω_0, where Δ changes sign, behave at $f \leq f_c$.

We found that the gap function at zero frequency, $\Delta(0)$, vanishes exponentially fast with $(f_c - f)$. The frequency ω_0 vanishes as well, but parametrically slower as $\sqrt{f_c - f}$. We argued that this parametrical difference between $\Delta(0)$ and ω_0 allows one to obtain a non-zero solution of the gap equation for all $f < f_c$. We note that the transition at f_c can be also interpreted from topological perspective, as the center of the dynamical vortex reaches $\omega = 0$ at $f = f_c$ and would have nowhere to go if superconductivity persisted above f_c.

We complimented the analysis of $\Delta(\omega)$ near f_c by the analysis of the propagator of phase fluctuations. We have shown that the superfluid density and the compressibility, which control momentum and frequency parts of the propagator of a phase field, deviate from the BCS values at a generic $f < f_c$, but tend to the BCS values at $f \to f_c$ and undergo a finite jump at $f = f_c + 0^+$. We showed that this, however, holds only for the superfluid density (and the compressibility) defined at strictly zero momentum. We introduced a generic momentum-dependent $n_s(\mathbf{q})$ and showed that it gradually vanishes at $f \to f_c$ for all $|v_F\mathbf{q}| > \Delta_0$. At f slightly below f_c, this behavior holds or all $|\mathbf{q}|$ except the ones which are exponentially small in $f_c - f$.

There are multiple possibilities to extend our analysis. One extension, which we leave for further research, is a potential coexistence of even-frequency and odd-frequency superconducting orders at $f \leq f_c$. Such a state spontaneously breaks time-reversal symmetry.

Finally, our analysis is not constrained to electron–phonon interaction and is applicable to all cases when there is a near-constant repulsion and frequency-dependent, retarded attraction due to a boson exchange. Other interesting candidates for a boson are exiton-polaritons in a microcavity[25,26] or cavity photons[27]. Experimental cavity setups often come with a tuning knob which allows one to change the relative strength of repulsive and attractive components of the interaction (i.e., continuously change f in our model). This should allow one to observe phase transition at f_c that we analyzed in this work.

METHODS

Derivation of n_s by expanding the action in θ

After the Hubbard-Stratonovich transformation is performed, the mixed boson-fermion action takes the form (for the following derivation, compare, e.g., ref. [28]):

$$\begin{aligned}
&\mathcal{S} = \mathcal{S}_\Delta - \textstyle\int_{p,p'} \overline{\Psi}_p G^{-1}(p,p')\Psi_{p'} \\
&\mathcal{S}_\Delta = \textstyle\int_q \int d\omega d\omega' \overline{\Delta}(\omega,q) V^{-1}(\omega-\omega')\Delta(\omega',q) \\
&\Psi_p = \left(c_\uparrow(p), \overline{c}_\downarrow(-p)\right)^T, \quad p = (\nu, \mathbf{p}) \\
&G^{-1}(p,p') = \begin{pmatrix} G_0^{-1}(p)\delta^{(d+1)}(p-p') & \Delta\left(\frac{1}{2}(\nu+\nu'), p-p'\right) \\ \overline{\Delta}\left(\frac{1}{2}(\nu+\nu'), p'-p\right) & -G_0^{-1}(-p)\delta^{(d+1)}(p-p') \end{pmatrix}.
\end{aligned} \tag{37}$$

Here, the first argument of Δ contains the relative energy, and the second the total energy-momentum of the Cooper pair, compare Fig. 4. Integrating out the fermions, we obtain a purely bosonic action

$$\mathcal{S} = \mathcal{S}_\Delta - \mathrm{Tr}\ln(-G^{-1}), \tag{38}$$

where the trace runs over energy-momenta and Nambu indices. From Eq. (38), the gap equation is simply derived by setting $\delta\mathcal{S}/\delta\Delta(\omega) = 0$. We look for mean-field solutions which have zero total energy-momentum, i.e., contain a delta-function $\delta^{(d+1)}(q)$.

To find the action of the Goldstone-mode, we insert the expansion from Eq. (22),

$$\begin{aligned}
\Delta(\omega,q) &\simeq \Delta(\omega) \times \left[\delta^{(d+1)}(q) + i\theta(q)\right] \\
\overline{\Delta}(\omega,q) &\simeq \Delta(\omega) \times \left[\delta^{(d+1)}(q) - i\theta(-q)\right],
\end{aligned} \tag{39}$$

into (38). The $\mathcal{O}(\theta^0)$ contribution from the $\mathcal{S}_\Delta$ term has the form

$$\int d\omega \Delta(\omega) V^{-1}(\omega-\omega')\Delta(\omega) \times \delta^{(d+1)}(0). \tag{40}$$

The term $\delta^{(d+1)}(0)$ should be interpreted as volume factor. The $\mathcal{O}(\theta)$-contribution cancels, and the $\mathcal{O}(\theta^2)$-contribution reads

$$S_\theta^{(a)} = \int_q \theta(q)\theta(-q)\left[\int \frac{d\omega d\omega'}{(2\pi)^2}\Delta(\omega)(-V^{-1})(\omega-\omega')\Delta(\omega')\right]. \tag{41}$$

To expand the $(\mathrm{Tr}\ln)$-term, it is convenient to split

$$\begin{aligned}
&G^{-1}(p,p') = G_0^{-1}(p,p') + X(p,p') \\
&G_0^{-1}(p,p') = \delta^{d+1}(p-p')\begin{pmatrix} i\nu - \xi_{\mathbf{p}} & \Delta(\nu) \\ \Delta(\nu) & i\nu - \xi_{-\mathbf{p}} \end{pmatrix} \\
&X(p,p') = \begin{pmatrix} 0 & \Delta\left(\frac{\nu+\nu'}{2}\right) i\theta(p-p') \\ -\Delta\left(\frac{\nu+\nu'}{2}\right) i\theta(p-p') & 0 \end{pmatrix}
\end{aligned} \tag{42}$$

Now, the trace of the logarithm can be expanded as

$$\begin{aligned}
\mathrm{Tr}\ln\left(-G^{-1}\right) &= \mathrm{Tr}\ln\left(-G_0^{-1}(1+G_0\cdot X)\right) \\
&= \mathrm{Tr}\ln\left(-G_0^{-1}\right) + \mathrm{Tr}(G_0\cdot X) - \tfrac{1}{2}\mathrm{Tr}(G_0\cdot X\cdot G_0\cdot X).
\end{aligned} \tag{43}$$

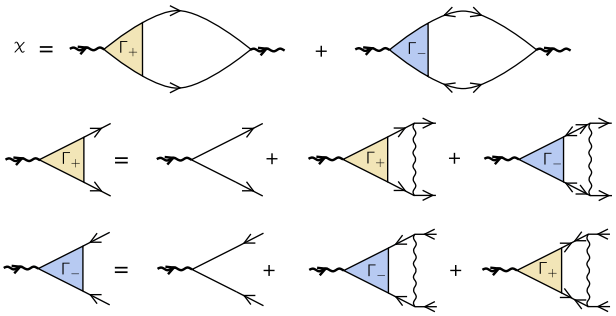

Fig. 7 Diagrammatic representation of χ. Straight lines with a single arrow represent normal fermion propagators G, lines with a double arrow anomalous propagators F. Thin wavy lines represent interactions V, thick wavy lines the pairing field Δ.

The first term is independent of θ, and the second term $\mathcal{O}(\theta)$ cancels. To evaluate the third term $\mathcal{O}(\theta^2)$, it is convenient to introduce center-of-mass coordinates as $(\Omega, \mathbf{q}) = q = p - p'$ and $(\omega, \mathbf{k}) = k = \frac{p+p'}{2}$. In these coordinates, $-\frac{1}{2}\mathrm{Tr}(G_0 \cdot X \cdot G_0 \cdot X)$ is

$$-\frac{1}{2}\int_{k,q} \mathrm{tr}\,[G_0(k+q/2)\cdot X(k+q/2,k-q/2)\cdot G_0(k-q/2)\cdot X(k-q/2,k+q/2)], \tag{44}$$

where tr acts in the spinor space. After straightforward algebra, the combination of this term and (41) yields $\mathcal{S}_\theta$ from the main text, Eq. (24).

Derivation of n_s from the particle–particle susceptibility

An alternative way of deriving the expressions for the superfluid density n_s and dynamical compressibility κ is by computing the full particle–particle susceptibility χ from Feynman diagrams. The basic building blocks for the diagrams are the normal and anomalous Green's functions,

$$\begin{aligned} G_{\alpha\beta}(\omega,\mathbf{k}) &= -\delta_{\alpha\beta}\frac{i\omega+\xi_{\mathbf{p}}}{\omega^2+\xi_{\mathbf{k}}^2+\Delta(\omega)^2}, \\ F_{\alpha\beta}(\omega,\mathbf{k}) &= i\sigma^y_{\alpha\beta}\frac{\Delta(\omega)}{\omega^2+\xi_{\mathbf{k}}^2+\Delta(\omega)^2}, \end{aligned} \tag{45}$$

where $\Delta(\omega)$ is chosen as real, α, β are spin indices, and σ^y is a Pauli matrix.

The pairing susceptibility $\chi(q)$ can be represented as the sum of two contributions containing renormalized vertices Γ_+, Γ_-, see Fig. 7. The vertices satisfy the two coupled Bethe-Salpeter equations and have poles corresponding to transverse (phase) fluctuations and longitudinal (Higgs) fluctuations (see e.g., ref. [29]). One can verify that to describe only phase fluctuations one has to take $\Gamma \equiv \Gamma_+ = -\Gamma_-$. The single equation for Γ then reads

$$\begin{aligned} \Gamma(\omega,q) &= 1 + \textstyle\int \frac{d\omega'}{2\pi}\Gamma(\omega',q)V(\omega-\omega')\times A(\omega',q), \\ A(\omega',q) &= \textstyle\int \frac{d\mathbf{k}}{(2\pi)^d}[G(\omega'+\Omega/2,\mathbf{k}+\mathbf{q}/2)G(-\omega'+\Omega/2,-\mathbf{k}+\mathbf{q}/2) \\ &\quad + F(\omega'+\Omega/2,\mathbf{k}+\mathbf{q}/2)F(-\omega'+\Omega/2,-\mathbf{k}+\mathbf{q}/2)]. \end{aligned} \tag{46}$$

Inserting the forms of G and F, Eq. (45), we find that $A(\omega, q)$ and the modified particle–particle bubble $\Pi_\Delta(\omega, q)$, introduced in Eq. (25), are related as

$$\Pi_\Delta(q) = \int \frac{d\omega}{2\pi} A(\omega,q)\Delta^2(\omega). \tag{47}$$

To solve Eq. (46), we make an ansatz

$$\Gamma(\omega,q) = \frac{\Phi(\omega,q)}{c_1|\mathbf{q}|^2 + c_2\Omega^2}, \tag{48}$$

where $\Phi(\omega, q)$ is regular and non-vanishing for $q = 0$, and c_1, c_2 are some constants. Then, $\Gamma(\omega, 0) = \infty$, which formally solves (46). To find the values of c_1 and c_2, we expand $A(\omega, q)$ from Eq. (46) in Ω, $|\mathbf{q}|$:

$$A(\omega,q) \simeq A(\omega,0) + a_{\mathbf{q}}(\omega)|\mathbf{q}|^2 + a_\Omega(\omega)\Omega^2. \tag{49}$$

Likewise, we expand

$$\Phi(\omega,q) \simeq \Phi(\omega,0) + \phi_{\mathbf{q}}(\omega)|\mathbf{q}|^2 + \phi_\Omega(\omega)\Omega^2. \tag{50}$$

The coefficients $A(\omega, 0)$, $a_{\mathbf{q}}$, a_Ω are known, while the coefficients $\Phi(\omega, 0)$, $\phi_{\mathbf{q}}$, ϕ_Ω, c_1, c_2 are not known. We substitute Eqs. (48), (49), and (50) into Eq. (46), which yields

$$\begin{aligned} &\Phi(\omega,0) + \phi_{\mathbf{q}}(\omega)|\mathbf{q}|^2 + \phi_\Omega(\omega)\Omega^2 = c_1|\mathbf{q}|^2 + c_2\Omega^2 + \\ &\textstyle\int \frac{d\omega'}{(2\pi)} V(\omega-\omega')\left[\Phi(\omega',0) + \phi_{\mathbf{q}}(\omega')|\mathbf{q}|^2 + \phi_\Omega(\omega')\Omega\right] \\ &\qquad \times \left[A(\omega',0) + a_{\mathbf{q}}(\omega')|\mathbf{q}|^2 + a_\Omega(\omega')\Omega^2\right]. \end{aligned} \tag{51}$$

We now compare the prefactors for $\mathcal{O}(1)$, $\mathcal{O}(|\mathbf{q}|^2)$, and $\mathcal{O}(\Omega^2)$ on both sides of this equation. At order $\mathcal{O}(1)$, we have

$$\Phi(\omega,0) = \int \frac{d\omega'}{2\pi} V(\omega-\omega')\Phi(\omega',0)A(\omega',0). \tag{52}$$

One can easily verify that the solution is $\Phi(\omega, 0) = \Delta(\omega)\gamma$, where γ is some constant, and $\Delta(\omega)$ is a solution of the gap equation. Comparing the prefactors for the $\mathcal{O}(|\mathbf{q}|^2)$-term, we get

$$\begin{aligned} \phi_{\mathbf{q}}(\omega) = c_1 &+ \textstyle\int \frac{d\omega'}{2\pi}\phi_{\mathbf{q}}(\omega')A(\omega',0)V(\omega-\omega') \\ &+ \textstyle\int \frac{d\omega'}{2\pi}\Phi(\omega',0)a_{\mathbf{q}}(\omega')V(\omega-\omega'). \end{aligned} \tag{53}$$

Multiplying (53) by $1/(2\pi)\times\Phi(\omega,0)A(\omega,0)$ and integrating over ω, we obtain

$$\begin{aligned} &\textstyle\int \frac{d\omega}{2\pi}\phi_{\mathbf{q}}(\omega)\Phi(\omega,0)A(\omega,0) = c_1 \int \frac{d\omega}{2\pi}\Phi(\omega,0)A(\omega,0) \\ &+ \textstyle\int \frac{d\omega'}{2\pi}\phi_{\mathbf{q}}(\omega')\Phi(\omega',0)A(\omega',0) + \int \frac{d\omega'}{2\pi}\Phi^2(\omega',0)a_{\mathbf{q}}(\omega'), \end{aligned} \tag{54}$$

where the gap equation in the form (52) was applied twice on the right-hand side of Eq. (54). Canceling the identical terms on both sides, we solve for c_1:

$$c_1 = -\frac{\gamma}{\int \frac{d\omega}{2\pi}\Delta(\omega)A(\omega,0)} \times \int \frac{d\omega}{2\pi}\Delta^2(\omega)a_{\mathbf{q}}(\omega). \tag{55}$$

In a similar fashion, we obtain

$$c_2 = -\frac{\gamma}{\int \frac{d\omega}{2\pi}\Delta(\omega)A(\omega,0)} \times \int \frac{d\omega}{2\pi}\Delta^2(\omega)a_\Omega(\omega). \tag{56}$$

Combining (55), (56), and (48), we obtain, to the leading order in Ω, $|\mathbf{q}|$,

$$\Gamma(\omega,q) \simeq \frac{\Phi(\omega,0)}{c_1|\mathbf{q}|^2 + c_2\Omega^2} = \frac{\Delta(\omega)\times \int \frac{d\omega'}{2\pi}\Delta(\omega')A(\omega',0)}{n_s|v_F\mathbf{q}|^2 + \kappa\Omega^2} \tag{57}$$

where

$$n_s = -\frac{1}{v_F^2}\int \frac{d\omega}{2\pi}\Delta(\omega^2)a_{\mathbf{q}}(\omega) \tag{58}$$

$$\kappa = -\int \frac{d\omega}{2\pi}\Delta^2(\omega)a_\Omega(\omega), \tag{59}$$

are the same as in the main text and in the previous section, see Eqs. (30) and (31). Note that an arbitrary constant γ has canceled out, as it indeed should. The susceptibility χ has the same pole structure as Γ. To the leading order in q we have

$$\chi(q) \simeq \int \frac{d\omega}{2\pi}\Gamma(q,\omega)A(\omega,0) = \frac{\left(\int \frac{d\omega}{2\pi}\Delta(\omega)A(\omega,0)\right)^2}{n_s|v_F\mathbf{q}|^2 + \kappa\Omega^2}. \tag{60}$$

DATA AVAILABILITY

The numerical data used in the analysis in this work are available upon request from the corresponding author.

CODE AVAILABILITY

The codes used to generate the numerical data are available upon request from the corresponding author.

Received: 13 December 2021; Accepted: 23 March 2022;
Published online: 19 April 2022

REFERENCES

1. Tolmachev, V. V. & Tiablikov, S. V. A new method in the theory of superconductivity. II. *Sov. Phys. JETP* **34**, 66 (1958).
2. Bogoljubov, N. N., Tolmachov, V. V. & Širkov, D. V. A new method in the theory of superconductivity. *Fortschr. Phys.* **6**, 605–682 (1958).
3. McMillan, W. L. Transition temperature of strong-coupled superconductors. *Phys. Rev.* **167**, 331–344 (1968).
4. Scalapino, D. J., Schrieffer, J. R. & Wilkins, J. W. Strong-coupling superconductivity. I. *Phys. Rev.* **148**, 263–279 (1966).
5. Morel, P. & Anderson, P. W. Calculation of the superconducting state parameters with retarded electron-phonon interaction. *Phys. Rev.* **125**, 1263–1271 (1962).
6. Carbotte, J. P. Properties of boson-exchange superconductors. *Rev. Mod. Phys.* **62**, 1027–1157 (1990).
7. Gurevich, V., Larkin, A. & Firsov, Y. A. Possibility of superconductivity in semiconductors. *Sov. Phys. Solid State* **4**, 131 (1962).
8. Rietschel, H. & Sham, L. J. Role of electron Coulomb interaction in superconductivity. *Phys. Rev. B* **28**, 5100–5108 (1983).
9. Ruhman, J. & Lee, P. A. Superconductivity at very low density: the case of strontium titanate. *Phys. Rev. B* **94**, 224515 (2016).
10. Ruhman, J. & Lee, P. A. Pairing from dynamically screened Coulomb repulsion in bismuth. *Phys. Rev. B* **96**, 235107 (2017).
11. Wölfle, P. & Balatsky, A. V. Superconductivity at low density near a ferroelectric quantum critical point: doped $SrTiO_3$. *Phys. Rev. B* **98**, 104505 (2018).
12. Chubukov, A., Prokof'ev, N. V. & Svistunov, B. V. Implicit renormalization approach to the problem of Cooper instability. *Phys. Rev. B* **100**, 064513 (2019).
13. Balatsky, A. V., Vekhter, I. & Zhu, J.-X. Impurity-induced states in conventional and unconventional superconductors. *Rev. Mod. Phys.* **78**, 373–433 (2006).
14. Abrikosov, A. & Gor'kov, L. On the theory of superconducting alloys. 1. The electrodynamics of alloys at absolute zero. *Sov. Phys. JETP* **8**, 1090–1098 (1959).
15. Abrikosov, A. & Gor'kov, L. Superconducting alloys at finite temperatures. *Sov. Phys. JETP* **9**, 220–221 (1959).
16. Skalski, S., Betbeder-Matibet, O. & Weiss, P. R. Properties of superconducting alloys containing paramagnetic impurities. *Phys. Rev.* **136**, A1500–A1518 (1964).
17. Christensen, M. H. & Chubukov, A. V. Dynamical vortices in electron-phonon superconductors. *Phys. Rev. B* **104**, L140501 (2021).
18. Wu, Y.-M., Zhang, S.-S., Abanov, A. & Chubukov, A. V. Interplay between superconductivity and non-Fermi liquid at a quantum critical point in a metal. IV. The γ model and its phase diagram at $1 < \gamma < 2$. *Phys. Rev. B* **103**, 024522 (2021).
19. Wu, Y.-M., Zhang, S.-S., Abanov, A. & Chubukov, A. V. Interplay between superconductivity and non-Fermi liquid behavior at a quantum-critical point in a metal. V. The γ model and its phase diagram: the case $\gamma = 2$. *Phys. Rev. B* **103**, 184508 (2021).
20. Damascelli, A. Probing the electronic structure of complex systems by ARPES. *Physica Scripta* **T109**, 61 (2004).
21. Bardeen, J. & Pines, D. Electron-phonon interaction in metals. *Phys. Rev.* **99**, 1140–1150 (1955).
22. Phan, D. & Chubukov, A. V. Effect of repulsion on superconductivity at low density. *Phys. Rev. B* **105**, 064518 (2022).
23. Eliashberg, G. Interactions between electrons and lattice vibrations in a superconductor. *Sov. Phys. JETP* **11**, 696–702 (1960).
24. Kusunose, H., Fuseya, Y. & Miyake, K. Possible odd-frequency superconductivity in strong-coupling electron–phonon systems. *J. Phys. Soc. Jpn.* **80**, 044711 (2011).
25. Laussy, F. P., Kavokin, A. V. & Shelykh, I. A. Exciton-polariton mediated superconductivity. *Phys. Rev. Lett.* **104**, 106402 (2010).
26. Cotleţ, O., Zeytinoğu, S., Sigrist, M., Demler, E. & Imamoğlu, A. Superconductivity and other collective phenomena in a hybrid Bose-Fermi mixture formed by a polariton condensate and an electron system in two dimensions. *Phys. Rev. B* **93**, 054510 (2016).
27. Schlawin, F., Cavalleri, A. & Jaksch, D. Cavity-mediated electron-photon superconductivity. *Phys. Rev. Lett.* **122**, 133602 (2019).
28. Altland, A. & Simons, B. D. *Condensed Matter Field Theory* (Cambridge University Press, 2010).
29. Cea, T., Barone, P., Castellani, C. & Benfatto, L. Polarization dependence of the third-harmonic generation in multiband superconductors. *Phys. Rev. B* **97**, 094516 (2018).

ACKNOWLEDGEMENTS

We thank Matthias Hecker, Dan Phan, Jörg Schmalian, and Shang-Shun Zhang for useful discussions. The work was supported by NSF grant DMR-1834856.

AUTHOR CONTRIBUTIONS

D.P. and A.V.C. performed the analytic calculations. D.P. performed the numerical computations. Both authors contributed to the discussion of results and to writing the manuscript.

COMPETING INTERESTS

The authors declare no competing interests.

ADDITIONAL INFORMATION

Correspondence and requests for materials should be addressed to Dimitri Pimenov.

Reprints and permission information is available at http://www.nature.com/reprints

Publisher's note Springer Nature remains neutral with regard to jurisdictional claims in published maps and institutional affiliations.